A Facile Route to Isotropic Conductive Nanocomposites by Direct Polymer Infiltration of Carbon Nanotube Sponges

Xuchun Gui,[†,‡] Hongbian Li,[§] Luhui Zhang,[§] Yi Jia,[‡] Li Liu,[‡] Zhen Li,[‡] Jinquan Wei,[‡] Kunlin Wang,[‡] Hongwei Zhu,[‡,*] Zikang Tang,[†] Dehai Wu,[‡] and Anyuan Cao[§,*]

[†]State Key Laboratory of Optoelectronic Materials and Technologies, School of Physics and Engineering, Sun Yat-Sen University, Guangzhou 510275, China, [‡]Key Laboratory for Advanced Materials Processing Technology and Department of Mechanical Engineering, Tsinghua University, Beijing 100084, China, and [§]Department of Advanced Materials and Nanotechnology, College of Engineering, Peking University, Beijing 100871, China

ABSTRACT Fabrication of high-performance nanocomposites requires that the nanoscale fillers be dispersed uniformly and form a continuous network throughout the matrix. Direct infiltration of porous CNT sponges consisting of a three-dimensional nanotube scaffold may provide a possible solution to this challenge. Here, we fabricated CNT sponge nanocomposites by directly infiltrating epoxy fluid into the CNT framework while maintaining the original network structure and CNT contact, with simultaneous improvement in mechanical and electrical properties. The resulting composites have an isotropic structure with electrical resistivities of 10 to 30 Ω · cm along arbitrary directions, much higher than traditional composites by mixing random CNTs with epoxy matrix. We observed reversible resistance change in the sponge composites under compression at modest strains, which can be explained by tunneling conduction model, suggesting potential applications in electromechanical sensors.

KEYWORDS: carbon nanotubes · sponges · nanocomposites · isotropic property · electromechanical device

Nanocomposites have wide applications as structural media, coatings for electrical or thermal management, and devices such as sensors and actuators.[1−5] To effectively enhance the mechanical and electrical properties, nanomaterial fillers such as carbon nanotubes (CNTs) are usually dispersed in polymer matrix uniformly with appropriate concentrations enabling percolation.[6−9] Even the composite is electrically percolated; there exist only limited conducting channels through overlapped CNT chains. It remains challenging to form continuous CNT networks across the entire matrix with minimal addition of fillers.[8,9] At the microscale, CNTs may be wrapped by polymeric molecules without forming direct contacts with adjacent tubes in the mixture, and the composite conductivity relying on the tunneling conduction through CNTs is generally several orders of magnitude lower than that in pure CNT networks.[10,11]

Distribution and morphology of CNTs within the composite matrix have been studied extensively. Uniform dispersion, suitable aspect ratios, and appropriate surface functionalities of CNTs are key factors for making high-performance nanocomposites. Formation of continuous CNT networks throughout the matrix is essential for simultaneously improving mechanical and electrical properties. To date, many methods have been developed to improve the dispersion of CNTs and interaction between CNTs and matrix, including solution mixing, chemical functionalization, *in situ* polymerization, infiltration, *etc.*,[12−17] with much progress in making conductive and reinforced nanocomposites.

More recently, vertical CNT forests and horizontally aligned CNT arrays have been incorporated into various polymers to make flexible and stretchable membranes, with potential applications in electromechanical sensors and actuators, electrical and thermal management, and filters.[17−22] In their methods, a polymeric fluid was infiltrated into the space among the forest/array and makes a membrane with CNTs extending continuously along the same direction. The mechanical properties and the electrical and thermal conductivity along the tube axis direction can be greatly enhanced due to the presence of long, continuous CNTs through the polymer matrix, although along the perpendicular direction, the enhancement is negligible.[16−18,23] Therefore, composites made by infiltration of aligned CNTs have an anisotropic structure and property. Furthermore, laminates can be made to

* Address correspondence to anyuan@pku.edu.cn, hongweizhu@tsinghua.edu.cn.

Received for review March 16, 2011 and accepted May 19, 2011.

Published online May 19, 2011
10.1021/nn201002d

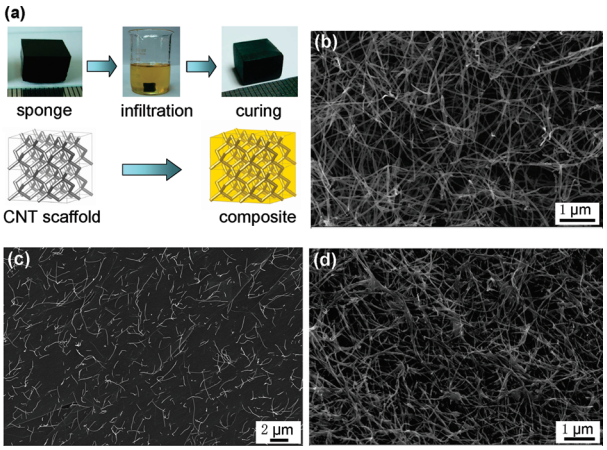

Figure 1. Fabrication and characterization of CNT sponge polymer composites. (a) Pictures of pristine monolithic CNT sponge, infiltrated and cured composites (top panel) and illustration of the polymer infiltration into a CNT scaffold (bottom panel). (b) SEM image of the pristine CNT sponge showing porous, scaffold-like morphology. (c) SEM image of the inner part in a broken composite showing complete filling by epoxy resin. (d) SEM image of the sponge composite after removal of epoxy, in which the original CNT network is preserved.

obtain isotropic two-dimensional structure, and an aligned CNT forest has been grown on a laminate surface to enhance through-thickness properties.[24] However, these composites still suffer from poor interlaminate interaction because the adhesion between the directly grown CNTs and the fiber substrate is not strong.

Recently, we reported porous CNT sponges whose structure is based on a three-dimensional (3D) interconnected CNT framework.[25] The sponges are stable under different stress conditions, such as compression, bending, and twisting, and can recover to original shape after significant deformation. In early applications, we demonstrated that these low density and flexible sponges can be squeezed repeatedly without collapsing, and they have an extremely huge ability to absorb oil molecules from the water surface by capillary action.[25,26] Such porous CNT sponges are very suitable for polymer infiltration and composite fabrication.

RESULTS AND DISCUSSION

Here, we use the CNT sponges as a template to infiltrate epoxy resin and fill the sponge pores completely, as illustrated in Figure 1a. As-grown sponges are hydrophobic and have an open pore structure, thus epoxy resin diluted in acetone can be directly introduced into the sponge (see Methods section for details). The size of the nanocomposite is decided by the origin sponges' size. Introduction of epoxy is carried out smoothly without disturbing the intrinsic structure and morphology of the sponge, and conducting paths *via* the CNT networks are preserved. The CNT scaffold, which can be synthesized and processed into any shape, determines the final composite shape (*e.g.*, a cubic block). Random distribution of CNTs makes it possible to reinforce the composites in all directions at the same time. The high porosity of sponges allows epoxy to occupy a substantial volume fraction (>99%) in the composite. To facilitate the infiltration of viscous fluid, the sponge was immersed into epoxy resin with a small addition of acetone, and then acetone was removed by vacuum heating (see Methods section). After complete curing, the composite maintains the same shape and overall size compared to the original sponge, indicating that there is little deformation or shrinkage occurring during the filtration process.

We characterized sponge and composite samples at different steps during infiltration (from original sponge to cured composite) by means of scanning electron microscopy (SEM) images. The original sponge contains numerous multiwalled CNTs (with diameters of ~30 nm and lengths of 10−50 μm) overlapped randomly into a thick carpet (Figure 1b). Unlike an aligned forest and array, the CNTs here show a random distribution, and the entire structure is isotropic. After filtration, we characterized the inner part of the cured composite by breaking the composite in liquid nitrogen. Epoxy resin has filled most of the empty space in the pristine sponge, and uniform, partially embedded CNTs were observed from the fractured surface (Figure 1c). It indicates that flowing of epoxy fluid into the sponge pores did not cause aggregation of CNTs. In order to check the network structure buried by epoxy, we washed away the epoxy matrix before it completely cured. SEM image reveals a network morphology resembling the original sponge, although some of the CNTs are wrapped by epoxy residue (Figure 1d). SEM results confirm that the epoxy-filled sponge composite has been made while maintaining CNT networks inside.

CNT sponges have been prepared in different porosities and densities (5−50 mg/cm^3). Therefore, the CNTs loading in the composites can be changed within

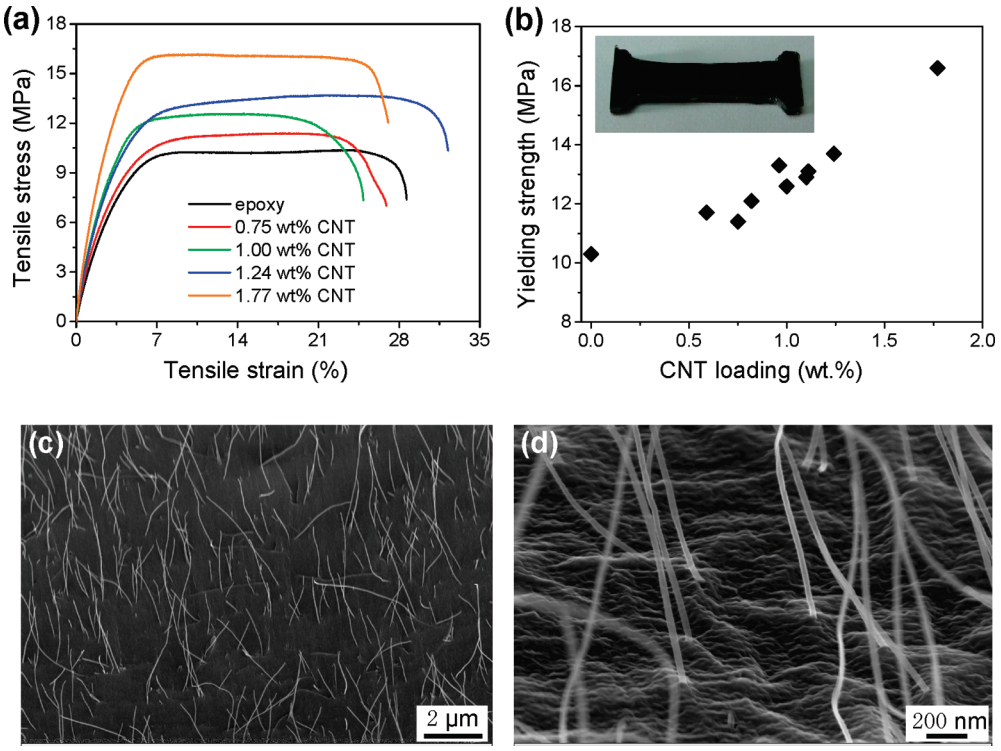

Figure 2. Reinforcement of composites by the CNT scaffold. (a) Tensile stress−strain curves of sponge composites with different CNT loadings (from 0.75 to 1.77 wt %). (b) Plots of yielding strengths of the composites *versus* CNT loading. Inset, picture of the test composite sample with 1 wt % CNTs. (c) SEM image of the fractured section after composite failure, showing CNT arrays pulled out from the epoxy matrix. (d) Enlarged view of (c) on CNTs embedded in the composite.

a certain range. Epoxy composites fabricated from CNT sponges with different densities (5−25 mg/cm^3) have CNT loadings from 0.75 to 1.77 wt % correspondingly (see Supporting Information Figure S1), and their mechanical properties (in tension) were studied. All stress−strain curves show a linear relationship at the initial stage of tensile loading, followed by a long plateau region, where yielding of epoxy occurred, and a sudden drop upon fracture (Figure 2a). Composites embedding a CNT scaffold show 10−60% enhancement in yielding strengths (about 16.1 MPa at 1.77 wt % of CNTs) compared with the control sample (pure epoxy, 10.3 MPa), in which the yielding strength increases linearly with the weight percentage of CNTs (Figure 2b). In comparison, random CNT−epoxy composites using functionalized multiwalled nanotubes show increase in tensile strength from 4.2 to 35%[27,28] and sometimes decrease in strength due to agglomeration of CNTs in the epoxy matrix.[29] The loading of CNTs seems to have only a small influence on the failure strain. SEM characterization reveals many individual CNTs exposed from the fractured area (Figure 2c). These CNTs became aligned along the tensile stress direction, indicating that they have been pulled out from the epoxy matrix during testing (Figure 2d). Uniform distribution of CNTs across the matrix is a critical factor for achieving higher mechanical strength at relatively low CNT concentrations (<2 wt %). However, since a large number of CNTs have been pulled out from the fractured section, we think the interaction between CNTs and epoxy matrix is not strong enough, and the intrinsic strength of CNTs has not been fully utilized. In our sponge composites, there are several factors contributing to the mechanical properties: the spatial density of CNTs (can be controlled by the CVD process), the length of individual CNTs, and the CNT−matrix interaction. Increasing the CVD reaction time produces thicker sponges (more number of CNTs), but the average CNT lengths remain in the range of several to tens of micrometers. Currently, the nanocomposites are made by infiltration of pristine sponges where CNT surfaces are not functionalized. Therefore, increasing loading (weight percentage) of CNTs could enhance the yielding strength, but to influence the failure strain, we need grow much longer CNTs with improved interaction with polymer matrix. Potential routes include synthesis of sponges with longer CNTs and appropriate chemical functionalization on the CNT surface.

We also measured electrical resistances of the sponge composites along different directions (inset of Figure 3a). Measurements were done by making composites in rectangular or cubic blocks and depositing electrodes to contact two opposite sides of a composite block. Current−voltage curves are recorded in the length, width, and thickness direction, all of

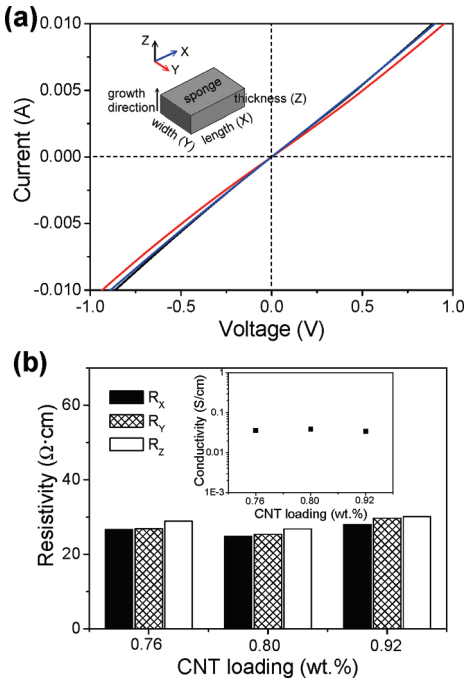

Figure 3. Isotropic electrical conductivity of the sponge composites. (a) Current−voltage (*I*−*V*) curves measured on a cubic composite (CNT loading 0.76 wt %) along three perpendicular directions, in which the growth direction is along the composite thickness (*Z*) and the length direction (*X*) is parallel with the gas flow during synthesis. (b) Resistivities measured from composites with varing CNT loadings, showing small fluctuation along different directions. Inset, calculated conductivities of the tested sponge composites.

which exhibit similar behavior (Figure 3a). Tests on three different samples show bulk resistivities in the range of 10 to 30 Ω·cm, and in each sample, the resistivities along three perpendicular directions are very close (Figure 3b). The isotropic electrical property of the composites is attributed to the three-dimensional CNT framework for molding composites. Also, low composite resistivity indicates that the interconnectedness and physical contacts between CNTs are well-maintained during epoxy infiltration. Pure epoxy blocks without CNTs are nearly insulating when measured under similar conditions (a current flow of less than 1×10^{-10} A under 1 V bias) (Supporting Information Figure S2). The conductivity of directly infiltrated sponge composites with the same CNTs loading (>10^{-2} S/cm) are 2−3 orders higher (inset of Figure 3b) in comparison with that (10^{-4}−10^{-5} S/cm) of traditional CNT−polymer composites prepared by solution mixing.[30−33]

Finally, we demonstrate that conductive epoxy−CNT sponge composites can act as electromechanical sensors under uniaxial compression. The composite sample shows certain flexibility and can be compressed within a modest strain range (<7%) and recover to original volume upon unloading (Figure 4a). Compressive stress−strain curves accompanied by simultaneous electrical measurement show a significant decrease of resistivity during the compression cycle, and the resistivity returns to the initial value at the end of the cycle. The composite shows a drop of resistivity (from about 17 to 10 Ω·cm) when it was compressed to a strain of $\varepsilon = 7\%$, due to the increased tunneling points between CNTs embedded in the epoxy matrix. Similar resistance change has been observed in several other CNT−polymer composites under compression or stretching.[17−19,22] Here, our sponge composite shows reversible resistance decrease (ΔR) relative to original value (R_0) over many cycles and maintains a roughly linear relationship *versus* strain in every cycle (Figure 4b). Irreversible compression strain and resistance changes occur only at relatively high strain levels.

The composite structure is stable under compression. When the sample was kept static for 30 s at a strain of 3 and 7%, the recorded resistivity remains nearly constant during the static periods (Figure 4c). We also fabricated a series of composite samples with a wide range CNT loadings (0.59 to 3.3 wt %) and compressed them in the same strain range (3−7%). We observed similar behavior in these composites, with relative decrease in resistance ($\Delta R/R_0$) in the range of 15 to 70%, as summarized in Figure 4d. Above a certain CNT loading (0.76 wt %), the value of $\Delta R/R_0$ decreases consistently with increasing CNT loading until 3.3 wt %. An optimal CNT content in the composite for maximum response to mechanical compression is found to be about 1 wt %.

There are three possible factors related to the movement of CNTs or bulk response underlying the observed conductivity change in the sponge composites, including (1) drop in contact numbers between embedded CNTs due to scissoring effect under compression where some CNTs are pulled apart (resulting in increase of resistance) and some are pushed together, (2) bulk compression response related to the material Poisson's ratio such as a slight change in sample cross-section size, and (3) reduced distance between polymer-wrapped CNTs that potentially leads to enhanced tunneling conduction between adjacent CNTs within a certain range. Because an overall decrease of resistance was observed experimentally and bulk response under compression remains modest, we suggest that the third factor (tunneling effect) is dominating here and is responsible for the significant conductivity change (by more than 40%). The resistance change ($\Delta R/R_0$) in the composite caused by tunneling effect can be related to the compressive strain (ε) based on the following model.

The electrical percolation of a CNT−epoxy composite is simplified as multiple paths consisting of a series of CNT interconnections through contacts (preserved during epoxy infiltration) and tunneling conduction

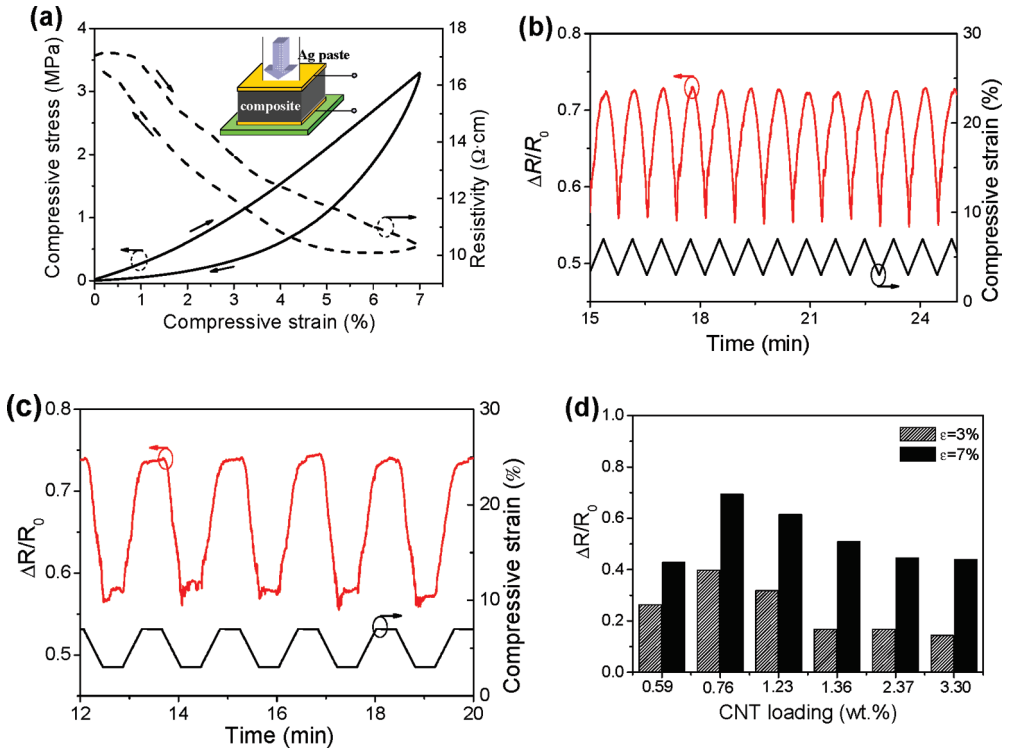

Figure 4. Electromechanical properties of the sponge composites. (a) Stress−strain curves and simultaneously recorded resistivity values by compressing a composite with 0.59 wt % CNTs (loading and unloading) at a maximum strain of 7%. Inset, illustration of the electromechanical test setup in which the top and bottom surfaces of the composite were coated by Ag paste contacts for resistivity measurements. (b) Time-resolved resistance change in relative to original value ($\Delta R/R_0$) recorded for a number of cycles at compressive strains between 3 and 7%. (c) Resistance change recorded during compression cycles in which the sample was kept stable for 30 s at maximum (7%) or minimum (3%) strains. (d) Calculated resistance changes for composites with different CNT loadings at predefined compressive strains (ε = 3 and 7%, respectively).

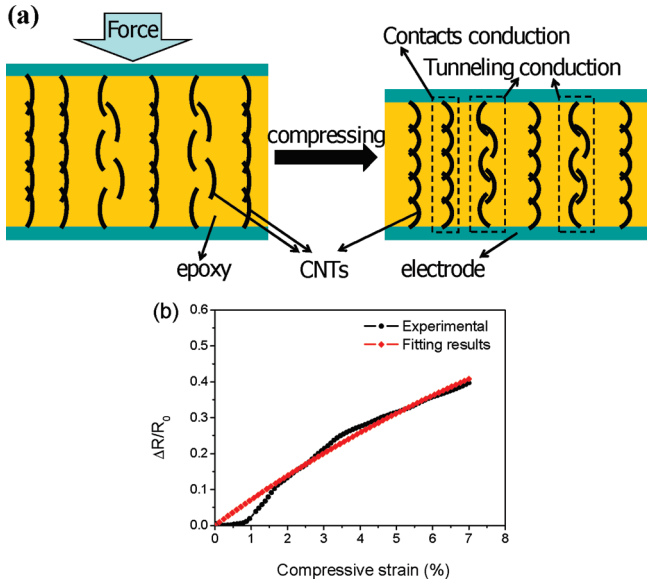

Figure 5. Analysis of conductivity change in the CNT−epoxy composite during compression. (a) Illustration of two typical conduction paths (direct CNT contacts and tunneling) through CNTs embedded in the sponge composite under uniaxial compression. (b) Experimental data acquired from compressing a sponge composite (with 0.59 wt % CNTs) and fitting results by the tunneling conduction model (eq 5).

joints between adjacent CNTs embedded in the matrix (illustrated in Figure 5a). In a path having contacts without or with a small distance, tunneling between CNTs becomes a bottleneck and can make

the path more conductive under appropriate compressive conditions.

In a nanocomposite containing randomly distributed nanoscale fillers in a polymeric host, the tunneling current (J) between two CNTs separated by a small distance (l) at low bias voltage (V) is determined by the following equation:[34,35]

$$J = \frac{3\sqrt{2m\varphi}}{2l}\left(\frac{e}{h}\right)^2 V \exp\left(-\frac{4\pi l}{h}\sqrt{2m\varphi}\right) \quad (1)$$

where m and e are the electron mass and charge, h is the Planck constant, and φ is the barrier height between two adjoining CNTs, which depends on the work functions of CNTs and epoxy.[34,35]

Under a constant bias and assuming an effective cross-section area producing the tunneling effect of a^2 and a total number of such junctions of n, the tunneling conduction resistance in a composite (R_m) is

$$R_m = n\frac{l\sqrt{2m\varphi}}{3a^2 m\varphi}\left(\frac{h}{e}\right)^2 \exp\left(\frac{4\pi l}{h}\sqrt{2m\varphi}\right) \quad (2)$$

When the distance between adjoining CNTs decreases from initially l_0 to an intermediate level of l during loading, correspondingly, the value of R_m changes from initially R_0 to R. To simplify, we only consider the relative resistance R/R_0, which is

$$\frac{R}{R_0} = \frac{l}{l_0}\exp\left[-\frac{4\pi}{h}\sqrt{2m\varphi}\times(l_0 - l)\right] \quad (3)$$

where l_0 is related to the weight percentage of CNTs in original sponge composites and therefore decided by the composite fabrication process.

Under uniaxial compression, CNTs may move apart or closer to each other depending on specific configurations. Only CNTs with reduced distance could form new tunneling points and contribute to the conductivity enhancement. Assuming a uniform mixture and homogeneous compression through the entire sponge composite, the distance between CNTs being compressed closer may be related to the compressive strain with a linear relationship as

$$l = l_0(1 - \varepsilon) \quad (4)$$

When eqs 3 and 4 are combined, the relative resistance change (reduction) due to tunneling conduction can be calculated by

$$\frac{\Delta R}{R_0} = \frac{R_0 - R}{R_0} = 1 - (1 - \varepsilon)\exp\left[-\frac{4\pi}{h}\sqrt{2m\varphi}\times l_0\varepsilon\right] \quad (5)$$

The fitting results by eq 5 are shown in Figure 5b, which accord well with the experimental results obtained from sponge composite with 0.76 wt % at compressive strains larger than 1%. A resistance decrease by about 40% was obtained at a modest compressive strain of 7%, and the conductivity change is fully reversible.

CONCLUSIONS

We reported an isotropic polymer composite made from infiltration of a self-assembled CNT sponge scaffold, with uniform CNT dispersion and well-preserved intertube contact. The sponge composites display isotropic electrical behavior, with improved and consistent conductivity along any direction. Electromechanical tests on composites with different CNT loadings show reversible and controllable resistivity change during compression cycles at modest strains. By filling the sponge pores with other selected polymers, we can make flexible membranes useful in optoelectronic and electromechanical devices. The fabrication method can be scaled up to produce much larger volume composites owing to the interconnected porous structure of CNT sponges. Our results demonstrate an alternative method for composite fabrication with uniform filler dispersion and reliable interfiller connection.

METHODS

Synthesis of CNT Sponges. The CNT sponges were directly synthesized by chemical vapor deposition (CVD) in a horizontal furnace. A quartz plate was placed in the middle of the reactor as growth substrate. The reaction temperature was set to 860 °C. Ferrocene and 1,2-dichlorobenzene were used as the catalyst precursor and carbon source, respectively. The carbon source solution with the ferrocene concentration of 0.06 g/mL was injected into the CVD reactor at a constant feeding rate in the range of 0.1−0.3 mL/min. A mixture of Ar and H_2 with the flowing rate of 2000 and 300 mL/min was used as carrier gas. After growth, the furnace was cooled to room temperature under the protection of Ar. The thickness of the CNT sponge increased with the growth time. A typical growth of 4 h produced a CNT sponge of ~8 mm thick.

Fabrication of the Composites. The epoxy resin (E-44, epoxide value = 0.41−0.47 equiv/100 g) was first dissolved in acetone at room temperature in a beaker. The curing agent (polyamide) was then added into the solution and uniformly mixed. The weight ratio of the epoxy resin, curing agent, and acetone was 2:1:1. The CNT sponge was completely immersed into the mixture solution. After infiltration for 15 min, the beaker was put in a vacuum oven to heat for 1 h to evaporate acetone away. Then, the sponge was picked up from the beaker and cured at 40 °C in the vacuum oven. Extra epoxy adhered on the sponge surface was removed before curing. The CNT loading in the composite was determined by measuring the weight of the CNT sponge before infiltration and the composite after epoxy infiltration.

Characterization of the Composites: Tensile and Electromechanical Test. The distribution and morphology of CNTs in the composites were characterized by a scanning electron microscope

(SEM, Leo 1530). Tensile test was carried out on Instron 5843 equipped with a 1 kN load cell. The specimens for the tensile test were made into a bone shape with a dimension of 25 mm (length) × 4 mm (width) × 3 mm (thickness). The gauge length was fixed to be 15 mm, and the extension rate was 2.0 mm/min. Electrical properties of the composites were characterized by a standard two-probe method using a source meter (Keithley 2400). The specimens for electrical measurements and electromechanical test were made into cubic (about 10 × 10 × 10 mm^3) or rectangular blocks. The surfaces of the specimen were polished by 1000 grit sandpaper and cleaned by deionized water to expose the fresh section with CNTs protruding out for electrical contact. A layer of Ag paste was uniformly pasted on two opposite sides along thickness, length, or width direction as electrode pairs. During the compressive tests, the top stage was set to move downward at a constant rate of 0.5 mm/min. The resistance of the composite was recorded simultaneously with stress–strain curves under a constant bias of 1.0 V.

Acknowledgment. This work is supported by National Science Foundation of China (NSFC) (Grant No. 51072092) and Tsinghua University Initiative Scientific Research Program (Grant No. 2009THZ02123). A.C. acknowledges funding from the Beijing City Natural Science Foundation program (Grant No. 8112017).

Supporting Information Available: SEM images of the sponge composites with different CNT loadings, electrical measurement of pure epoxy samples. This material is available free of charge *via* the Internet at http://pubs.acs.org.

REFERENCES AND NOTES

1. Aliev, A. E.; Oh, J.; Kozlov, M. E.; Kuznetsov, A. A.; Fang, S.; Fonseca, A. F.; Ovalle, R.; Lima, M. D.; Haque, M. H.; Gartstein, Y. N.; *et al.* Giant-Stroke, Superelastic Carbon Nanotube Aerogel Muscles. *Science* **2009**, *323*, 1575–1578.
2. Gao, L.; Thostenson, E. T.; Zhang, Z.; Chou, T. Sensing of Damage Mechanisms in Fiber-Reinforced Composites under Cyclic Loading Using Carbon Nanotubes. *Adv. Funct. Mater.* **2009**, *19*, 123–130.
3. Zhang, Q.; Zhao, M.; Tang, D.; Li, F.; Huang, J.; Liu, B.; Zhu, W.; Zhang, Y.; Wei, F. Carbon-Nanotube-Array Double Helices. *Angew. Chem., Int. Ed.* **2010**, *49*, 3642–3645.
4. Coleman, J. N.; Khan, U.; Gun'Ko, Y. K. Mechanical Reinforcement of Polymers Using Carbon Nanotubes. *Adv. Mater.* **2006**, *18*, 689–706.
5. Spitalsky, Z.; Tasis, D.; Papagelis, K.; Galiotis, C. Carbon Nanotube–Polymer Composites: Chemistry, Processing, Mechanical and Electrical Properties. *Prog. Polym. Sci.* **2010**, *35*, 357–401.
6. Grossiord, N.; Loos, J.; Laake, L.; Maugey, M.; Zakri, C.; Koning, C. E.; Hart, A. J. High-Conductivity Polymer Nanocomposites Obtained by Tailoring the Characteristics of Carbon Nanotube Fillers. *Adv. Funct. Mater.* **2008**, *18*, 3226–3234.
7. Ajayan, P. M.; Tour, J. M. Nanotube Composites. *Nature* **2007**, *447*, 1066–1068.
8. Li, J.; Ma, P. C.; Chow, W. S.; To, C. K.; Tang, B. Z.; Kim, J. Correlations between Percolation Threshold, Dispersion State, and Aspect Ratio of Carbon Nanotubes. *Adv. Funct. Mater.* **2007**, *17*, 3207–3215.
9. Jeon, K.; Lumata, L.; Tokumoto, T.; Steven, E.; Brooks, J.; Alamo, R. G. Low Electrical Conductivity Threshold and Crystalline Morphology of Single-Walled Carbon Nanotubes—High Density Polyethylene Nanocomposites Characterized by SEM, Raman Spectroscopy and AFM. *Polymer* **2007**, *48*, 4751–4764.
10. Zhang, R.; Baxendale, M.; Peijs, T. Universal Resistivity–Strain Dependence of Carbon Nanotube/Polymer Composites. *Phys. Rev. B* **2007**, *76*, 195433.
11. Xiao, H.; Li, H.; Ou, J. Modeling of Piezoresistivity of Carbon Black Filled Cement-Based Composites under Multi-axial Strain. *Sens. Actuators, A* **2010**, *160*, 87–93.
12. Wardle, B. L.; Saito, D. S.; Garcia, E. J.; Hart, A. J.; Villoria, R. G.; Verploegen, E. A. Fabrication and Characterization of Ultrahigh-Volume-Fraction Aligned Carbon Nanotube–Polymer Composites. *Adv. Mater.* **2008**, *20*, 2707–2714.
13. Ma, W.; Liu, L.; Zhang, Z.; Yang, R.; Liu, G.; Zhang, T.; An, X.; Yi, X.; Ren, Y.; Niu, Z.; *et al.* High-Strength Composite Fibers: Realizing True Potential of Carbon Nanotubes in Polymer Matrix through Continuous Reticulate Architecture and Molecular Level Couplings. *Nano Lett.* **2009**, *9*, 2855–2861.
14. Yang, Z.; Cao, Z.; Sun, H.; Li, Y. Composite Films Based on Aligned Carbon Nanotube Arrays and a Poly(*N*-isopropyl acrylamide) Hydrogel. *Adv. Mater.* **2008**, *20*, 2201.
15. Zeng, H. L.; Gao, C.; Wang, Y. P.; Watts, P. C. P.; Kong, H.; Cui, X. W.; Yan, D. Y. *In Situ* Polymerization Approach to Multiwalled Carbon Nanotubes-Reinforced Nylon 1010 Composites: Mechanical Properties and Crystallization Behavior. *Polymer* **2006**, *47*, 113–122.
16. Cheng, Q. F.; Wang, J. P.; Wen, J. J.; Liu, C. H.; Jiang, K. L.; Li, Q. Q.; Fan, S. S. Carbon Nanotube/Epoxy Composites Fabricated by Resin Transfer Molding. *Carbon* **2010**, *48*, 260–266.
17. Jung, Y. J.; Kar, S.; Talapatra, S.; Soldano, C.; Viswanathan, G.; Li, X.; Yao, Z.; Ou, F. S.; Avadhanula, A.; Vajtai, R.; *et al.* Aligned Carbon Nanotube–Polymer Hybrid Architectures for Diverse Flexible Electronic Applications. *Nano Lett.* **2006**, *6*, 413–418.
18. Shin, M. K.; Oh, J.; Lima, M.; Kozlov, M. E.; Kim, S. J.; Baughman, R. H. Elastomeric Conductive Composites Based on Carbon Nanotube Forests. *Adv. Mater.* **2010**, *22*, 2663.
19. Lee, D. H.; Kim, J. E.; Han, T. H.; Hwang, J. W.; Jeon, S.; Choi, S.; Hong, S. H.; Lee, W. J.; Ruoff, R. S.; Kim, S. O. Versatile Carbon Hybrid Films Composed of Vertical Carbon Nanotubes Grown on Mechanically Compliant Graphene Films. *Adv. Mater.* **2010**, *22*, 1247.
20. Hu, Y.; Chen, W.; Lu, L.; Liu, J.; Chang, C. Electromechanical Actuation with Controllable Motion Based on a Single-Walled Carbon Nanotube and Natural Biopolymer Composite. *ACS Nano* **2010**, *4*, 3498–3502.
21. Sekitani, T.; Noguchi, Y.; Hata, K.; Fukushima, T.; Aida, T.; Someya, T. A Rubberlike Stretchable Active Matrix Using Elastic Conductors. *Science* **2008**, *321*, 1468–1472.
22. Zhang, Y.; Sheehan, C. J.; Zhai, J.; Zou, G.; Luo, H.; Xiong, J.; Zhu, Y. T.; Jia, Q. X. Polymer-Embedded Carbon Nanotube Ribbons for Stretchable Conductors. *Adv. Mater.* **2010**, *22*, 3027–3031.
23. Ci, L.; Suhr, J.; Pushparaj, V.; Zhang, X.; Ajayan, P. M. Continuous Carbon Nanotube Reinforced Composites. *Nano Lett.* **2008**, *8*, 2762–2766.
24. Veedu, V. P.; Cao, A.; Li, X.; Ma, K.; Soldano, C.; Kar, S.; Ajayan, P. M.; Ghasemi-Nejhad, M. N. Multifunctional Composites Using Reinforced Laminae with Carbon Nanotube Forests. *Nat. Mater.* **2006**, *5*, 457–462.
25. Gui, X.; Wei, J.; Wang, K.; Cao, A.; Zhu, H.; Jia, Y.; Shu, Q.; Wu, D. Carbon Nanotube Sponges. *Adv. Mater.* **2010**, *22*, 617–621.
26. Gui, X.; Cao, A.; Wei, J.; Li, H.; Jia, Y.; Li, Z.; Fan, L.; Wang, K.; Zhu, H.; Wu, D. Soft, Highly Conductive Nanotube Sponges and Composites with Controlled Compressibility. *ACS Nano* **2010**, *4*, 2320–2326.
27. Montazeri, A.; Khavandi, A.; Javadpour, J.; Tcharkhtchi, A. Viscoelastic Properties of Multi-walled Carbon Nanotube/Epoxy Composites Using Two Different Curing Cycles. *Mater. Des.* **2010**, *31*, 3383–3388.
28. Hou, Y.; Tang, J.; Zhang, H.; Qian, C.; Feng, Y.; Liu, J. Functionalized Few-Walled Carbon Nanotubes for Mechanical Reinforcement of Polymeric Composites. *ACS Nano* **2009**, *3*, 1047–1062.
29. Breton, Y.; Désarmot, G.; Salvetat, J. P.; Delpeux, S.; Sinturel, C.; Béguin, F.; Bonnamy, S. Mechanical Properties of Multiwall Carbon Nanotubes/Epoxy Composites: Influence of Network Morphology. *Carbon* **2004**, *5*, 1027–1030.
30. Yuen, S. M.; Ma, C. C. M.; Wu, H. H.; Kuan, H. C.; Chen, W. J.; Liao, S. H.; Hsu, C. W.; Wu, H. L. Preparation and Thermal, Electrical, and Morphological Properties of Multiwalled Carbon Nanotube and Epoxy Composites. *J. Appl. Polym. Sci.* **2007**, *103*, 1272–1278.

31. Liu, L.; Etika, K. C.; Liao, K. S.; Hess, L. A.; Bergbreiter, D. E.; Grunlan, J. C. Comparison of Covalently and Noncovalently Functionalized Carbon Nanotubes in Epoxy. *Macromol. Rapid Commun.* **2009**, *30*, 627–632.
32. Spitalsky, Z.; Krontiras, C. A.; Georga, S. N.; Galiotis, C. Effect of Oxidation Treatment of Multiwalled Carbon Nanotubes on the Mechanical and Electrical Properties of Their Epoxy Composites. *Composites, Part A* **2009**, *40*, 778–783.
33. Barrau, S.; Demont, P.; Perez, E.; Peigney, A.; Laurent, C.; Lacabanne, C. Effect of Palmitic Acid on the Electrical Conductivity of Carbon Nanotubes−Epoxy Resin Composites. *Macromolecules* **2003**, *36*, 9678–9680.
34. Yi, X.; Song, Y.; Zheng, Q. A Preliminary Study on Mechanical−Electrical Behavior of Graphite Powder-Filled High-Density Polyethylene Composites. *J. Appl. Polym. Sci.* **2000**, *77*, 792–796.
35. Xiao, H.; Li, H.; Ou, J. Modeling of Piezoresistivity of Carbon Black Filled Cement-Based Composites under Multi-axial Strain. *Sens. Actuators, A* **2010**, *160*, 87–93.